Search for Extra Scalars Produced in Association with Muon Pairs at the ILC

Yan Wang[◇*]**, Jenny List**[◇]**, Mikael Berggren**[◇]

◇ *DESY, Notkestraße 85, 22607 Hamburg, Germany*
* *IHEP, 19B Yuquan Road, Shijingshan District, Beijing, China*
E-mail: yan.wang@desy.de

on behalf of the International Large Detector concept group

We study the search for an extra scalar *S* boson produced in association with the *Z* boson at the International Linear Collider (ILC). The study is performed at center-of-mass energies of 250 GeV and 500 GeV based on the full simulation of the International Large Detector (ILD). In order to be as model-independent as possible, the analysis uses the recoil technique, in particular with the *Z* boson decaying into a pair of muons. As a result, exclusion cross-section limits are given in terms of a scale factor *k* with respect to the Standard Model Higgs-strahlung process cross section. These predicted results, covering all possible searching regions of the extra scalars at the 250 GeV ILC and the 500 GeV ILC, can be interpreted independently of the decay modes of the *S* boson.

1. Introduction

The motivation of our study is to find a new scalar *S* boson in the *SZZ* coupling since one or more extra scalars are predicted in many new physics models. However, the properties of 125 GeV scalar measured at the LHC is very similar to the Standard Model (SM) Higgs boson [1]. As a result, the new scalar's coupling will be highly suppressed [2]. Furthermore, the LEP/LHC constraints on the extra scalars always rely on the model details. Thus, a more precise analysis with model-independent assumptions to a scalar with the small coupling is preferred. Although the OPAL collaboration has searched for light scalars (less than 100 GeV) in a model-independent way at LEP, the results are limited by the low luminosity [3]. The International Linear Collider (ILC) is a proposed electron-positron linear collider, whose luminosity will be over a thousand times higher than that of LEP, which makes the recoil mass technique more accurate to find such extra scalars [4]. And the ILC has higher center-of-mass energies, which will cover more searching regions for the extra scalar. A preliminary version of this analysis has been reported at LCWS2017 [5] and ICHEP2018 [6]. Thus, only the updates from ICHEP2018 is summarized in this contribution.

2. Event Generation and Detector Simulation

The signal is $e^+e^- \to S + Z$ production, where the *Z* boson decays to a pair of muons. The decay branching ratios of *S* are fixed as same as the 125 GeV Higgs boson, but no use would be made of this fact. As SM backgrounds, bremsstrahlung and initial state radiation (ISR) are explicitly considered for all events. The event samples are generated with 100% left-handed and right-handed beam polarization, using the Whizard 1.95 Monte Carlo (MC) event generator [7]. Then the samples are reweighted with beam polarizations of $\pm 80\%$ for the electron beam and $\pm 30\%$ for the positron beam.

The event samples are generated, simulated and reconstructed for different center-of-mass energies ($\sqrt{s} =$250 GeV and 500 GeV). In 250 GeV cases, we use the same setting as the samples generated in the context of the ILD Detailed Baseline Design document [8]. The fractions of integrated luminosity 2000 fb^{-1} are dedicated to the four sign combinations $(-+, +-, ++, --) = (45\%, 45\%, 5\%, 5\%)$. The signal benchmark points are chosen as every 5 GeV in the range of $10 \leq M_S \leq 160$ GeV (totally 30 signal benchmark points). In 500 GeV cases, we use the samples generated in the context of the ILD Design Report [9], the fractions of integrated luminosity 4000 fb^{-1} are dedicated to $(-+, +-, ++, --) = (40\%, 40\%, 10\%, 10\%)$. Totally 48 signal benchmark points are chosen in the range of $10 \leq M_S \leq 410$ GeV. Event reconstruction has been performed using the PandoraPFA algorithm to reconstruct individual final state particles, so-called Particle Flow Objects (PFOs).

2.1 Event selection and Background Rejection

Firstly, a pair of oppositely charged muons is selected by minimizing the following χ^2 function:

$$\chi^2(M_{\mu^+\mu^-}, M_{\text{rec}}) = \frac{(M_{\mu^+\mu^-} - M_Z)^2}{\sigma^2_{M_{\mu^+\mu^-}}} + \frac{(M_{\text{rec}} - M_S)^2}{\sigma^2_{M_{\text{rec}}}} \tag{2.1}$$

37 where $M_{\mu^+\mu^-}$ and M_{rec} are the invariant mass and the recoil mass of the muon pair, and $\sigma_{M_{\mu^+\mu^-}}$

38 and $\sigma_{M_{\text{rec}}}$ are determined by a Gaussian fit to the generator-level distributions of $M_{\mu^+\mu^-}$ and

39 M_{rec}. Then, the bremsstrahlung and final state radiation photons from the muon are combined

40 with the muon.

41   Background events are rejected by firstly considering kinematic variables only relied on muons

42 (and the reconstructed Z boson): the invariant mass and transverse momentum of the muon pair, as

43 well as the polar angle of the missing momentum. Then, a BDTG is trained using 6 input variables

44 based on TMVA [10]: muon pair invariant mass, the polar angle of each muon, the polar angle

45 of the muon pair, the opening angle of the muon pair, and the $\pi - (\phi_{\mu^+} - \phi_{\mu^-})$, where $\phi_{\mu^\pm}$ is

46 the azimuthal angles of the muons with respect to the beam line. Finally, taking into account the

47 ISR photon return effects, the two fermion background can be further rejected by ISR energy veto

48 cuts. With these cuts, no information on the decay of S is needed, thus the expected results will be

model-independent. The recoil mass distributions are obtained after these cuts (Figure 1).
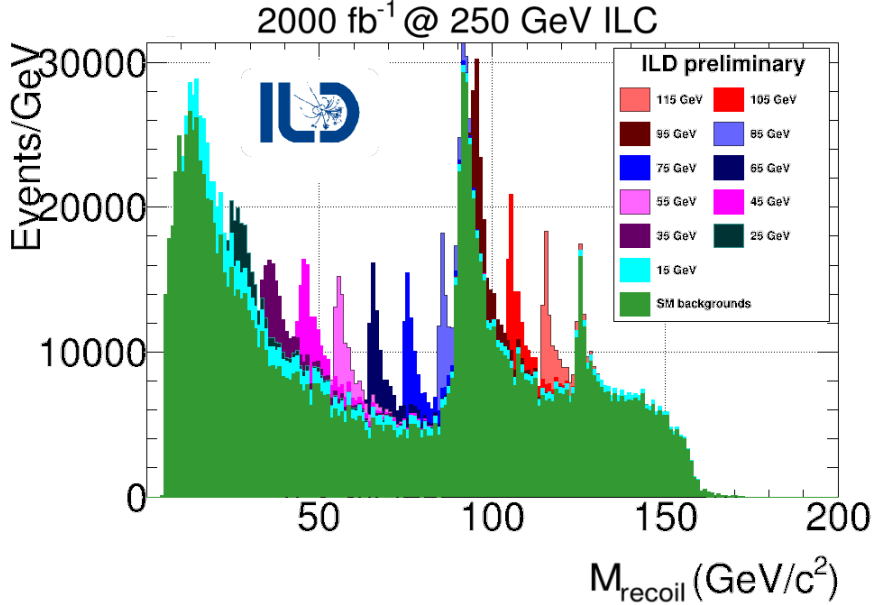

Figure 1: The recoil mass distributions for signal and backgrounds at the 250 GeV center of mass energy. These distributions are before the ISR veto cuts.

49

50 3. Results

51   A likelihood analysis is applied for calculating $2\,\sigma$ expected exclusion limits on k with a bin-

52 by-bin comparison between the signal and background recoil mass histograms for each benchmark

53 points, where k is defined as

$$k = \frac{\sigma_{SZ}}{\sigma_{H_{SM}Z}(m_{H_{SM}} = m_S)}. \tag{3.1}$$

54 , and k_{95} is the $2\,\sigma$ exclusion limits for the cross section scale factor k hereinafter.

55   In Figure 2, the ILC results at 250 GeV are compared with the LEP results directly. The red

56 points are $2\,\sigma$ exclusion limits for $\int L dt = 2000$ fb^{-1} and $\sqrt{S} = 250$ GeV at the ILC, while the red

57 line was obtained with the recoil mass method by the OPAL Collaboration [3] at LEP with about

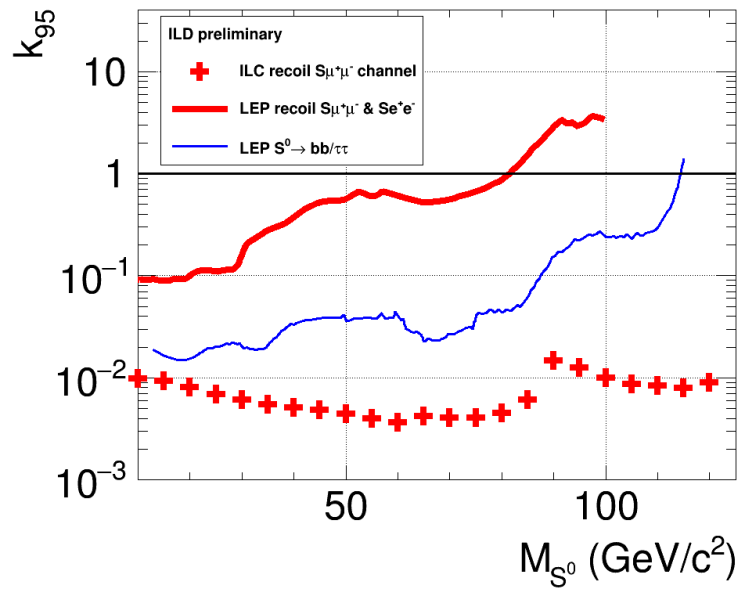**Figure 2:** The directly comparison between the LEP and ILC simulation results.
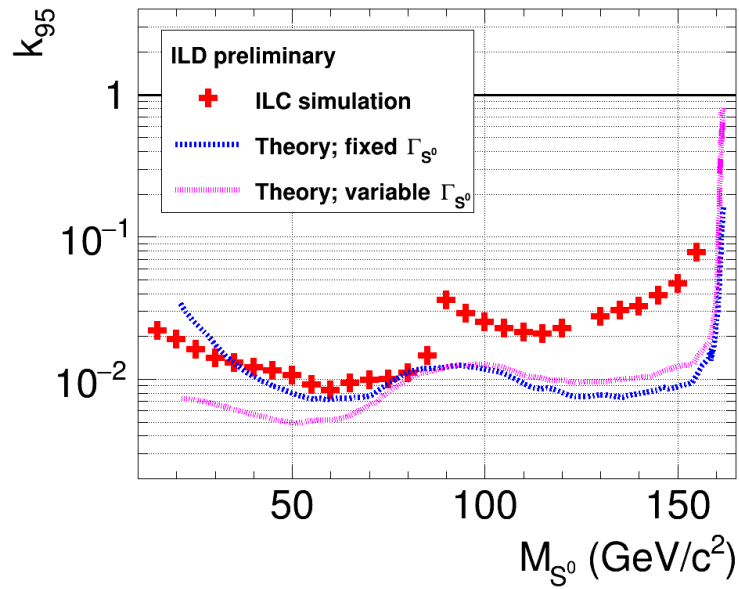

Figure 3: The comparison between the theoretical LEP extroplation results and ILC expected results.

58 0.8 fb^{-1} data in total. Also shown with the blue line is the model-dependent results from LEP,
59 combining measurements by ALEPH, DELPHI, L3, and OPAL [11], in which the decay modes of
60 the scalars were utilized. In general, the ILC exclusion limits will reach 10^{-2}, and are one or two
61 orders better than the OPAL recoil results and even better than the LEP traditional results.

62 In Figure 3, the ILC theoretical predictions, which are extrapolated from the LEP measure-
63 ments with fixed (variable) scalar width, are compared with the ILC simulation results [12]. The
64 theoretical predictions combine $S\mu^+\mu^-$ and Se^+e^- channels, while the ILC simulation results
65 only use $S\mu^+\mu^-$ channel, but divide the results by $\sqrt{2}$ ($k_{95} = k_{95}^{exp}(S\mu^+\mu^-)/\sqrt{2}$). These results
66 are projected with 500 fb^{-1} luminosity with $P(e^-, e^+) = (-80\%, +30\%)$. From the figure, the
67 ILC simulation results agree to the theoretical predictions with fixed scalar width in the low mass
68 region. However, the theoretical predictions extrapolate the expected background events in an in-
69 terval around the *Z* pole region [12], so there is no *Z* pole peak in the theoretical curves; at the same
70 time, the theoretical predictions don't include SM Higgs background, as a result, they are better
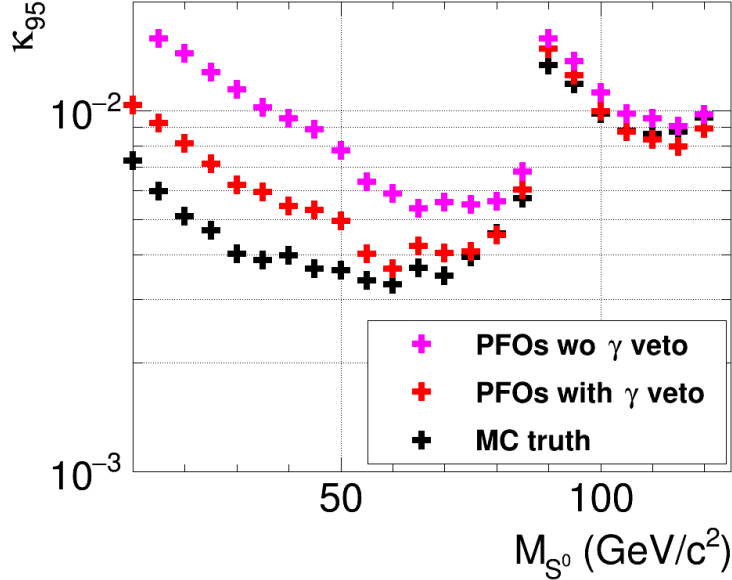than simulation results in the high mass region.

Figure 4: The effects for ISR photon veto cuts and the reconstruction efficiency.

71

72 In Figure 4, a comparison is given among the PFO and their corresponding MC simulation
73 inputs (MCtruth). The red and magenta points are the results with/without the ISR photon veto
74 cuts on the level of PFOs, because the two fermion background can be efficiently discarded by
75 considering the ISR effects. Thus, the ISR photon reconstructed efficiency will affect the result
76 significantly. The black points are the results after photon veto cuts using MCtruths with the detec-
77 tor simulation, which reflect the best searching capability. And the difference between MCtruths
78 and PFOs results shows we can improve the results with better photon reconstructions.

79 In Figure. 5, we show the preliminary exclusion limits for the 500 GeV ILC. In the low mass
80 region, the 500 GeV results are worse than the 250 GeV cases mainly due to the suppressed cross
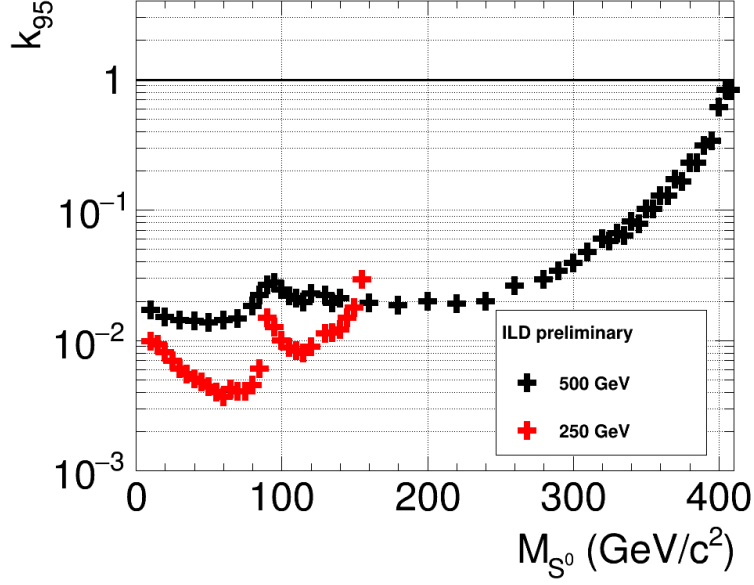
Figure 5: Preliminary Final Exclusion Limits for 250/500 GeV ILC.

sections, while they cover a larger searching region. Especially when $M_S < 300$ GeV, k_{95} is in the order of 10^{-2}, which could set strong model-independent constraints for the extra scalars.

4. Conclusions

By applying the recoil technique, the potential of the ILC to search for scalars has been investigated at $\sqrt{S} = 250$ GeV and 500 GeV, with the full simulation of the ILD concept. The method is optimized to be independent of the scalar decay modes. $2\,\sigma$ expected exclusion limits for the cross section scale factor k_{95} are shown for scalar mass from 10 GeV to 160 GeV when $\sqrt{S} = 250$ GeV and from 10 GeV to 410 GeV when $\sqrt{S} = 500$. They are one or two orders of magnitudes more sensitive than LEP, and covering substantial new phase spaces.

References

[1] The ATLAS and CMS collaboration, "Measurements of the Higgs boson production and decay rates and constraints on its couplings from a combined ATLAS and CMS analysis of the LHC pp collision data at $\sqrt{S} = 7$ and 8 TeV", JHEP 08 (2016) p.045.

[2] R. Aggleton et al., "Review of LHC experimental results on low mass bosons in multi Higgs models", JHEP 02 (2017) p. 035.

[3] G. Abbiendi , "Decay mode independent searches for new scalar bosons with the OPAL detector at LEP", Eur. Phys. J. C27 (2003) p. 311-329.

[4] D. M. Asner et al., "ILC Higgs Wh ite Paper", Proceedings, CSS2013 (2013) Minneapolis, USA, July 29-August 6, 2013.

[5] Y. Wang, J. List,and M. Berggren, "Search for Light Scalars Produced in Association with Muon Pairs for $\sqrt{s}$ = 250 GeV at the ILC", arXiv:1801.08164 [hep-ex].

[6] Y. Wang, J. List,and M. Berggren, "Search for Light Scalars Produced in Association with a *Z* boson at the 250 GeV stage of the ILC", ICHEP2018 Proceeding, PoS(ICHEP2018) 630.

[7] W. Kilian, T. Ohl and J. Reuter, "WHIZARD: Simulating Multi-Particle Processes at LHC and ILC", Eur. Phys. J. C **71**, 1742 (2011).

[8] H. Abramowicz et al., "The International Linear Collider Technical Design Report", ILC-REPORT-2013-040.

[9] ILD Detector Collaboration, "ILD Design Report" (2019).

[10] TMVA home page https://root.cern/tmva.

[11] R. Barate et al., "Search for the standard model Higgs boson at LEP", Phys. Lett. B565 (2003) p. 61-75.

[12] P. Drechsel, G. Moortgat-Pick, and G. Weiglein, "Sensitivity of the ILC to light Higgs masses", arXiv:1801.09662[hep-ph].